



Bombyx mori nucleopolyhedrovirus Bm46 is essential for efficient production of infectious BV and nucleocapsid morphogenesis



Yang Li ^{a,b}, Jianjia Zhang ^a, Xiangshuo Kong ^a, Nan Chen ^a, Xiaoqun Zeng ^a, Xiaofeng Wu ^{a,b,*}

^a College of Animal Sciences, Zhejiang University, Hangzhou 310058, PR China

^b Key Laboratory of Silkworm and Bee Resource Utilization and Innovation of Zhejiang Province, Hangzhou, PR China

ARTICLE INFO

Keywords:

BmNPV
Bm46
VP39
Nucleocapsid
ODV occlusion

ABSTRACT

Bombyx mori nucleopolyhedrovirus (BmNPV) orf46 (*Bm46*), the orthologues of *Autographa californica* multiple nucleopolyhedrovirus (AcMNPV) ac57, is a highly conserved gene in group I and group II nucleopolyhedroviruses (NPVs). However, its function in viral life cycle is unclear. Our results indicated that *Bm46* transcript was detected from infected cells at 12 h post infection, while *Bm46* protein was detectable from 24 to 72 h post infection. Upon the deletion of *Bm46*, fewer infectious BVs were produced by titer assays, but neither viral DNA synthesis nor occlusion bodies (OBs) production was affected. Electron microscopy revealed that *Bm46* knockout interrupted nucleocapsid assembly and occlusion-derived virus (ODV) embedding, resulting in aberrant capsid-like tubular structures accumulated in the RZ (ring zone). Interestingly, this abnormally elongated capsid structures were consistent with the immunofluorescence microscopy results showing that VP39 assembled into long filaments and cables in the RZ. Moreover, DNA copies decreased by 30 % in occlusion bodies (OBs) produced by *Bm46*-knockout virus. qRT-PCR and Western blot analysis showed that the expression of VP39 was affected by *Bm46* disruption. Taken together, our findings clearly pointed out that *Bm46* played an important role in BV production and the proper formation of nucleocapsid morphogenesis.

1. Introduction

The family *Baculoviridae* encompasses a diverse group of insect-specific viruses with circular double-stranded DNA genomes ranging from 80 to 180 kb in size(Herniou et al., 2003), packaged within enveloped, rod-shaped nucleocapsids(Hayakawa et al., 1999). There are four genera of *Baculoviridae*: *Alphabaculovirus* (lepidopteran nucleopolyhedrovirus [NPV]), *Betabaculovirus* (lepidopteran granulovirus [GV]), *Gammabaculovirus* (hymenopteran NPV), and *Deltabaculovirus* (dipteran NPV)(Jehle et al., 2006). The *Alphabaculovirus* genus falls into two phylogenetic clades, representing group I and group II NPVs(Herniou et al., 2001). In the infection cycle, the VS (virogenic stroma) region (an intranuclear viral replication center), is formed. Viral DNA replication and late gene transcription occur in the electron-dense VS. In the late phase of infection, viral DNA is condensed and packaged into capsids to form nucleocapsids within the VS. During viral infection, baculoviruses produce two types of virions, the budded virus (BV) and

occlusion-derived virus (ODV)(Rohrmann, 2013), each plays a critical role in the biology of the virus. One phenotype, the budded virus (BV), bud from the plasma membrane, is in charge of spreading the infection within susceptible tissues or among cells in culture. The occlusion-derived virus (ODV), occluded within a crystallized protein, initiates primary infection in the midgut epithelia of infected insects and thus is required for horizontal transmission among insect hosts. The major difference between BV and ODV is that BV obtains its envelope by budding viral modified protein areas of the plasma membrane, whereas the ODV envelope is derived from the inner nuclear membrane within a peripheral area, called the ring zone(Braunagel and Summers, 2007).

Bombyx mori nucleopolyhedrovirus (BmNPV) is the major pathogen of the silkworm, which leads to severe losses in the silk industry(Miao et al., 2005). The BmNPV genome is approximately 128 kb long with a G + C content of 40 % and 143 open reading frames (ORFs)(Gomi et al., 1999). The genomic sequence of the *Bm46* gene predicts a gene product of 161 amino acid residues with a putative molecular weight of

Abbreviations: B.mori, Bombyx mori; BmNPV, Bombyx mori nucleopolyhedrovirus; AcMNPV, *Autographa californica* multiple nucleopolyhedrovirus; HearNPV, *Helicoverpa armigera* nucleopolyhedrovirus; E.coli, *Escherichia coli*; ODV, occlusion-derived virus; OB, occlusion body; BV, budded virus; VS, virogenic stroma; RZ, ring zone; CT, capsid-like tubule structure; NC, nucleocapsid; NE, nuclear envelope; PH, polyhedrin.

* Corresponding author.

E-mail address: wuxiaofeng@zju.edu.cn (X. Wu).

<https://doi.org/10.1016/j.virusres.2020.198145>

Received 22 July 2020; Received in revised form 18 August 2020; Accepted 23 August 2020

Available online 1 September 2020

0168-1702/© 2020 Elsevier B.V. All rights reserved.

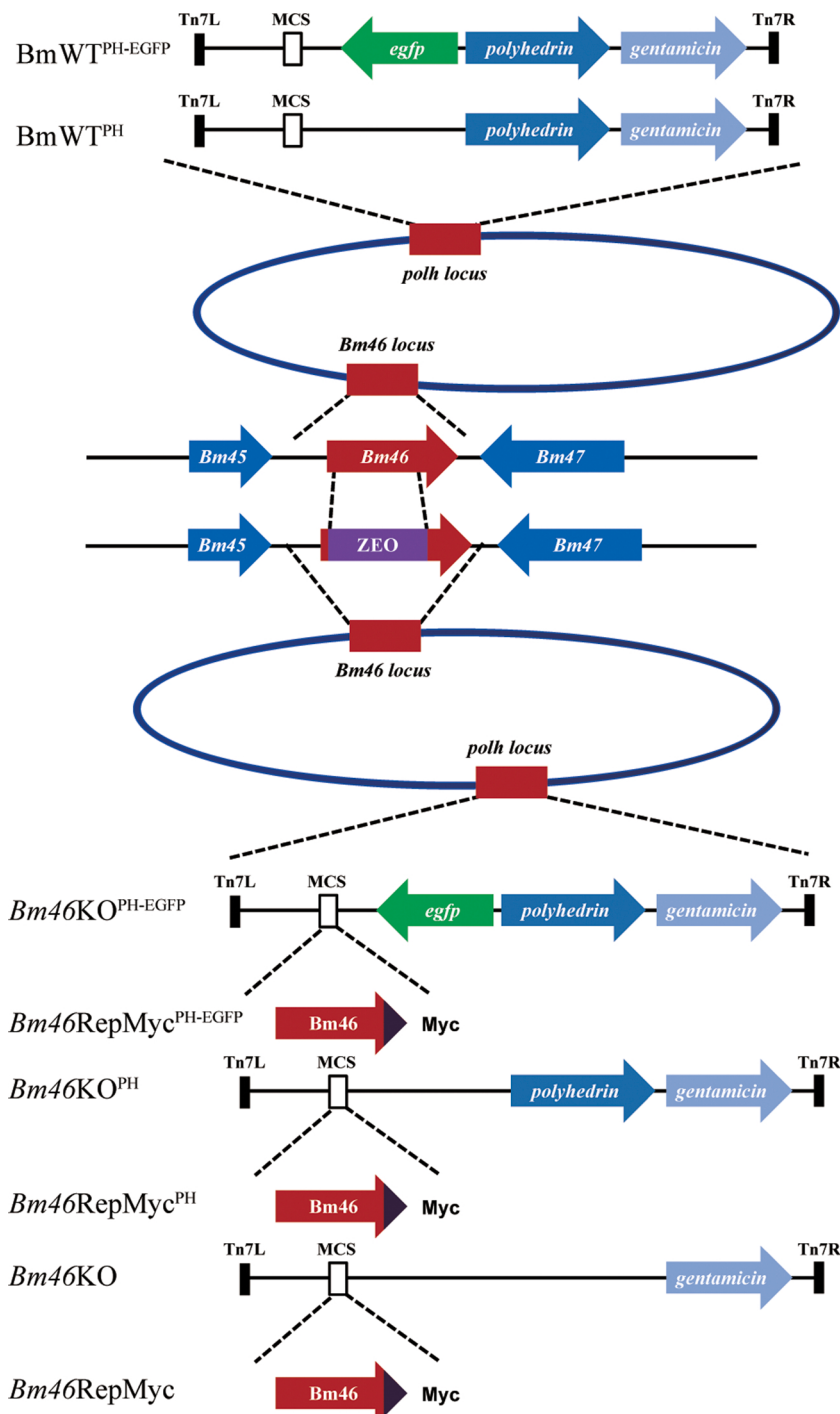


Fig. 1. Construction and characterization of wild-type, *Bm46* knockout and *Bm46* repaired BmNPV bacmids. Strategy for the construction of the recombinant viruses wild-type, *Bm46KO* and repair bacmids. *BmWT^{PH}* and *BmWT^{PH-EGFP}* were constructed to serve for positive control. The *Bm46* deletion mutant possesses a Zeocin resistance (ZEO) cassette in place of *Bm46* (open reading frame nucleotides 107 to 361). The following diagram shows the fragments inserted into the *polh* locus to generate *Bm46KO^{PH-EGFP}* and *Bm46KO^{PH}*. Similarly, with its native promoter and Myc-tagged at the C terminus, the repaired bacmid (*Bm46RepMyc^{PH-EGFP}*, *Bm46RepMyc^{PH}* and *Bm46RepMyc*) was constructed.

20.7 kDa. BmNPV orf46 (*Bm46*) is a highly conserved gene in almost all sequenced alphabaculovirus genomes. A series of gene knockout BmNPV mutants for each of 141 genes were constructed, which showed that *Bm46* gene was not required for infectious BV production(Ono et al., 2012). A more recent study showed that *Helicoverpa armigera* nucleopolyhedrovirus (HearNPV) *Ha50*, the *Bm46* ortholog, was regarded as an auxiliary gene as it played an uncertain role in the viral life cycle(Chen et al., 2012). However, the high conservation of *Bm46* in all sequenced group I and group II NPVs may suggest it plays an important role in the viral life cycle.

In this study, a *Bm46*-knockout virus (*Bm46KO*) was generated to further investigate the role of *Bm46* in the BmNPV life cycle. This

Bm46KO had different phenotypes from those described in the previous studies. Essentially, our results demonstrated that the deletion of *Bm46* reduced BV production and affected ODV occlusion. In addition, immunofluorescence assays showed that VP39 mislocalized into filaments and cables punctate in RZ of *Bm46KO*-transfected cells, and aberrant elongated tubular structures was visualized by TEM. In conclusion, our findings indicated that *Bm46* played a pivotal role in BV production and revealed the importance of *Bm46* in nucleocapsid assembly and morphogenesis.

2. Materials and methods

2.1. Insects, cell lines, viruses

Bombyx mori (*B. mori*) larvae were reared on mulberry at 25 °C. BmN cells were cultured at 27 °C in TC-100 insect medium supplemented with 10 % fetal bovine serum, 100 µg/mL penicillin, and 30 µg/mL streptomycin. The *Escherichia coli* strains BW25113 containing BmNPV genome was used to extract the Bacmid template. The T3 strain of BmNPV was used as WT virus(Maeda et al., 1985).

2.2. Construction of the *Bm46* knockout bacmid

The BmNPV *Bm46* gene was replaced by a Zeocin resistance (ZEO) gene through homologous recombination in *Escherichia coli* as described previously(Chartier et al., 1996; Hanahan, 1983). The cassette of ZEO gene was amplified using primers *Bm46KO-F* and *Bm46KO-R* from plasmid pIZ/V5-His. The fragment of ZEO cassette was generated containing the Zeocin gene (ZEO) flanked by 50 nt fragments homologous to the upstream and downstream regions of the *Bm46* ORF respectively, which is to mediate ZEO gene insertion into the *Bm46* locus while concomitantly deleting the *Bm46* ORF. The PCR fragment was gel purified and electroporated into *E. coli* BW25113 competent cells harboring the BmNPV bacmid and the helper plasmid pKD46. Positive clones were selected with Zeoncin/Kanamycin and further verified by PCR (supplementary Fig. 1) and sequencing. The PCR screening primers are listed in supplementary Table S1. The resulting bacmid was named *Bm46KO*.

2.3. Construction of the *Bm46* knockout, the repair, and wild-type bacmids containing polyhedrin or egfp

To visualize any defective effect for the mutation of *Bm46KO*, a series of donor vectors were constructed based on plasmid pFB1-PH-EGFP and pFB1-PH, which was constructed by inserting *polh* (*polyhedrin*) and *egfp* (*enhanced green fluorescence protein*) into pFastBI under the control of *polh* promoter and *ie1* promoter, respectively. A 784 bp fragment of *Bm46* cassette containing native *Bm46* gene with its own promoter and Myc tag in the C terminus region was PCR amplified from BmNPV genome (supplementary Table S1). Then, the fragment was cloned into pFB1-PH-EGFP and pFB1-PH plasmid to generate pFB1-*Bm46Myc-PH-EGFP* and pFB1-*Bm46Myc-PH*. After that, competent DH10Bm46KO cells were transformed with donor plasmids pFB1-PH-EGFP, pFB1-PH, pFB1-*Bm46Myc-PH-EGFP* and pFB1-*Bm46Myc-PH* to generate *Bm46*-null bacmid and *Bm46* repair bacmid using Bac-to-Bac system(Luckow et al., 1993), respectively (Fig. 1). DH10B cells containing pMON7124 helper plasmid and BmNPV genome were transformed with pFB1-PH-EGFP to generate a positive control bacmid named BmWT^{PH-EGFP}. Recombination products were then confirmed by PCR with primer M13.

2.4. One-step growth curve analysis

BmN cells (1×10^6) were transfected with 1.0 µg of each bacmid (BmWT^{PH-EGFP}, *Bm46KO*^{PH-EGFP}, *Bm46RepMyc*^{PH-EGFP}) using the Cellfectin liposome reagent. At designated time points, cell supernatants were collected and BV production was determined based on a 50 % tissue culture infective dose (TCID₅₀) endpoint dilution assay in BmN cells. In addition, BmN cells (1×10^6) were infected with the above viruses at an MOI of 1. At virous time points infection, the infected supernatants were collected and the titers were determined by TCID₅₀ assays.

2.5. Quantitative analysis of viral DNA synthesis

To assess viral DNA replication, a quantitative real time PCR (qRT-PCR) assay was performed as previously described(Vanarsdall et al.,

2005). BmN cells (1×10^6) were transfected in triplicates with 2 µg of positive control bacmid recombinant bacmid (BmWT^{PH-EGFP}), *Bm46* knockout bacmid (*Bm46KO*^{PH-EGFP}), or repaired bacmid DNA were collected at different time points. Total intracellular DNA was extracted with Universal Genomic DNA Extraction kit (TaKaRa) and resuspended in 50 µL of sterile water. Next, 20 µL of total DNA from each time point was digested with 20 units *Dpn*I (TaKaRa) overnight in a 40 µL reaction volume to eliminate the input bacmid DNA. Purified DNA sample was subjected to Quantitative Real-time PCR targeting *gp41* gene of BmNPV with primer pairs shown in supplementary Table S1.

2.6. Immunofluorescence microscopy and F-actin staining

Immunofluorescence assays were performed as described previously with some modifications(Yuan et al., 2011). Briefly, BmN cells (1×10^6) were seeded into 35-mm glass-bottom culture dishes and incubated at 27 °C for 12 h, followed by infection with *Bm46RepMyc* at an MOI of 1. At the indicated time points, cells were fixed in 4% paraformaldehyde for 15 min., and permeabilized with 0.1 % TritonX-100 for 10 min.. For immunofluorescence assays, cells were blocked in 5% BSA (bovine serum albumin in PBS), and incubated with mouse anti-Myc antibody (1:200, Invitrogen), mouse anti-β-actin (1:200, Beyotime) or rabbit anti-VP39 (1:200, Sigma) overnight. Cells were washed thrice in blocking buffer for 10 min. each time, subsequently incubated with a fluorescence-tagged antibody for 1 h. Samples incubated with Myc or β-actin antibody were further incubated with tetramethylrhodamine isocyanate (TRITC) goat anti-mouse antibody (Invitrogen) at a dilution of 1:200. Samples incubated with rabbit anti-VP39 antibody were further incubated with fluorescein isothiocyanate (FITC)goat anti-rabbit antibody at a dilution of 1:200. For F-actin staining, cells were incubated with Phalloidin-FITC at room temperature inside a covered container for 20 min.. The cells were then sealed in 4',6'- diamidino-2-phenylindole (DAPI) (Beyotime) for 10 min. in dark, and examined with a ZEISS LSM 780 confocal laser scanning microscopy. The fluorescence intensity was analyzed using Image J (National Institutes of Health).

2.7. Transmission electron microscopy

For transmission electron microscopy (TEM), BmN cells (1×10^6) were transfected with 2 µg of BmWT, *Bm46KO* and *Bm46RepMyc* bacmid DNA. At 96 h post-transfection (p.t.), cells were collected with a cell scraper and pelleted at 5000 rpm for 5 min.. Cells were then fixed, dehydrated, embedded, sectioned and stained as described previously. The blocks were viewed under a Hitachi Model SU8010 transmission electron microscope (TEM) operating at 80 kV. To analyze the content of ODV embedded in OB of BmWT^{PH} and *Bm46KO*^{PH}, 200 µL of purified OBs suspension (1×10^8 OBs/mL) from infected fifth-instar *B. mori* larvae were treated and viewed by TEM as mentioned above.

2.8. Western blot analysis

For time course analysis of protein expression, BmN cells (1×10^6) were seeded into 35-mm dishes, infected with the *Bm46RepMyc* at an MOI of 1, and collected at 0, 6, 12, 24, 36, 48, and 72 h p.i.. Cells were lysed in cell lysis buffer [20 mM Tris PH7.5, 150 mM NaCl, 1% Triton X-100, 2.5 mM sodium pyrophosphate, 1 mM EDTA, 1% Na₃VO₄, 0.5 µg/mL leupeptin, 1 mM phenylmethanes DNA synthesisulfonyl fluoride (PMSF)] (Beyotime) for 30 min. on ice, as described previously(Xu et al., 2019). Before subjected to 15 % sodium dodecyl sulfate-polyacrylamide gel electrophoresis (SDS-PAGE), an equal volume of 2×protein loading buffer (Beyotime) was added and boiled for 10 min.. The proteins were then transferred to polyvinylidene fluoride (PVDF) membrane, blocked in 5% non-fat milk, and incubated overnight at 4 °C with the following antibodies: anti-Myc (Invitrogen), anti-VP39 (M2; Sigma), anti-α-tubulin (Beyotime). After incubation with horseradish peroxidase (HRP)-conjugated secondary antibodies, membranes were developed by

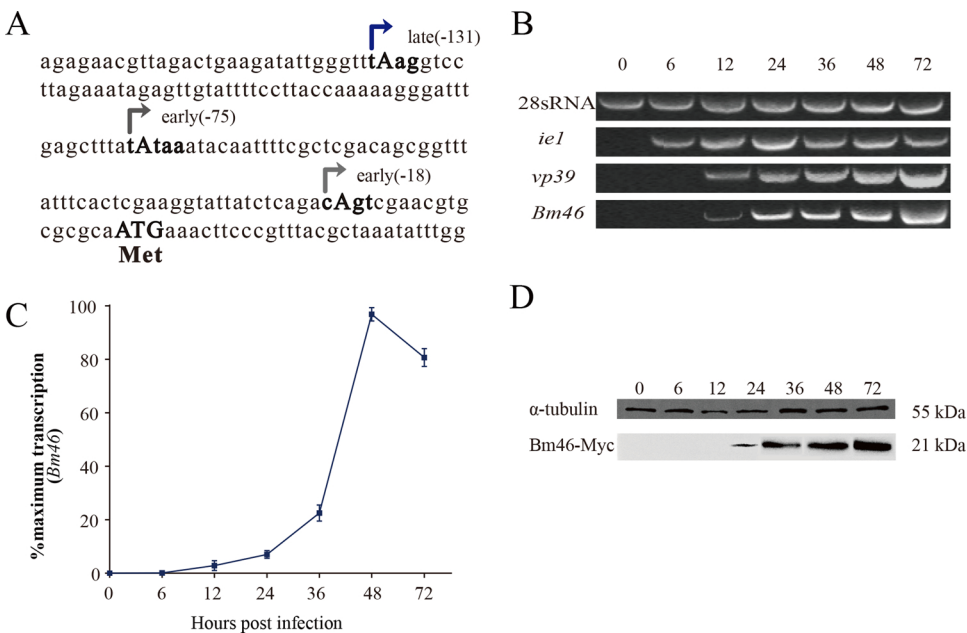


Fig. 2. Time-course analysis of BmNPV Bm46 transcription and expression. (A) Transcription start sites of *Bm46* transcripts. A previous transcriptomic study displayed that *Bm46* is transcribed from both early (TATAA or CAGT) and late (TAAG) motifs (Chen et al., n.d.), which are located upstream from and at transcript start sites respectively. (B, C) Temporal expression of *Bm46* mRNA. BmN cells were infected with *BmWT^{PH}* at an MOI of 1. At indicated time points, cells were harvested and total RNA was extracted. After total RNA reverse transcription, cDNA was subjected to qRT-PCR. The 28sRNA served as an internal control. (D) Western blot analysis of the *Bm46* expression profile. BmN cells were infected with *Bm46RepMyc* at an MOI of 1 and harvested at the various time points, lysed, boiled and subjected to Western blot using an anti-Myc antibody. Host protein α-tubulin was used as controls.

enhanced chemiluminescence. To examine the effect of *Bm46* deletion on the expression of major nucleocapsid protein VP39, BmN cells were infected with *BmWT^{PH}* or *Bm46KO^{PH}* at an MOI of 1. At various indicated time points, cells were harvested and lysed. Protein concentration in lysates was measured by BCA Protein Assay Kit (Takara). Next, 20 μg protein samples were mixed with 2× protein loading buffer (Beyotime) and subjected to western blot. α-tubulin was served as an internal reference.

2.9. qRT-PCR

BmN cells (1×10^6) were infected with *BmWT^{PH}*, *Bm46KO^{PH}* or *Bm46RepMyc^{PH}* at an MOI of 1. At the indicated time points, the cells were harvested and total RNA was extracted using RNAiso Plus (TaKaRa) according to the manufacturer's instructions. First-strand cDNAs were synthesized from 2 μg of total RNA by EasyScript® One-Step gDNA Removal and cDNA Synthesis SuperMix (TransGen Biotech). Quantitative Real-time PCR was performed using Hieff® qPCR SYBR® Green Master Mix (Yeasen) with primer pairs shown in supplementary Table S1, as described above. Reactions were carried out for 95 °C for 5 min and 40 cycles of 95 °C for 10 s and 60 °C for 30 s.

2.10. OB production from infected BmN cells

To quantify polyhedra release from infected BmN cells, 35-mm plate were seeded with BmN cells (1×10^6), cells were allowed to attach for 6 h, and then they were infected with *BmWT^{PH}*, *Bm46KO^{PH}* and *Bm46RepMyc^{PH}* at an MOI of 1. After 168 h p.i., medium was removed from each pellet. The pellets were washed with PBS, 0.1 % (m/v) SDS and 0.1 M NaCl in turn. Finally, the polyhedra released was quantified using a bacterial counting chamber.

2.11. OB production from infected larvae and DNA extraction

To produce and purify OBs, fifth-instar larvae were reared at 25°C, and were injected with 10 μl BV supernatant of *BmWT^{PH}*, *Bm46KO^{PH}* and *Bm46RepMyc^{PH}* using microinjector. The OBs obtained from homogenized infected cadavers were extracted and filtered through cheesecloth. After a few rounds of differential centrifugation followed by sucrose density gradient ultracentrifugation, the OBs were purified. Next, OBs (1×10^6) were digested with *Dpn* I to eliminate bacmid DNA

from *E. coli*. And then, OBs were lysed and virions were released by mixing 100 μl of 0.5 M Na₂CO₃ and 50 μl of 10 % SDS (sodium dodecyl sulfate) in a final volume of 500 μl for 10 min. at 60 °C (Simón et al., 2008). Undissolved OBs and other debris were removed by low-speed centrifugation and the supernatant containing virions was further treated with 25 μl of Proteinase K (TaKaRa, 20 mg/mL) for 30 min. at 50 °C. Viral DNA was extracted using the phenol-chloroform method, further being isolated by alcohol precipitation. The DNA concentration was estimated at 260 nm by Nanodrop (Thermo).

In addition, to quantify genomic DNA from OBs, qRT-PCR analysis was performed targeting *gp41* gene to represent the relative viral genome copies. Briefly, the viral genome DNA extracted from 5×10^8 OBs was used as template. qRT-PCR was performed to compare the viral genome DNA from OBs.

3. Results

3.1. Construction of the *Bm46* knockout and repaired BmNPV bacmids

To investigate the role of *Bm46* in viruses derived from BmNPV bacmid, a *Bm46*-knockout bacmid was constructed using RecE/RecT (ET) homologous recombination in *Escherichia coli* as described previously (Lin and Blissard, n.d.). The *Bm46* locus was replaced by a zeocin resistance cassette (ZEO) (Fig. 1). The recombinant Bacmid clones were screened by PCR to determine the success of *Bm46* disruption by ZEO. To investigate the effect of *Bm46* deletion on viral infection, we inserted the *polyhedrin* (*polh*) and *enhanced green fluorescence protein* (*EGFP*) gene simultaneously or *polh* singly into polyhedrin locus Tn7-mediated transposition to generate *Bm46KO^{PH-EGFP}* and *Bm46KO^{PH}* respectively. The repair bacmids *Bm46RepMyc^{PH-EGFP}*, *Bm46RepMyc^{PH}* and *Bm46RepMyc*, which contained the *Bm46* ORF driven by its native promoter with a Myc-encoding sequence at the C terminus, were constructed to confirm the observed knockout phenotypes. In addition, *BmWT^{PH-EGFP}* and *BmWT^{PH}* were also generated as positive controls. Two pairs of primer, rep-F/zeo-R and zeo-F/rep-R (supplementary table S1.), were used to confirm the recombination junctions of the upstream and downstream flanking regions, generating 961 bp and 745 bp fragments respectively (supplementary Fig. 1).

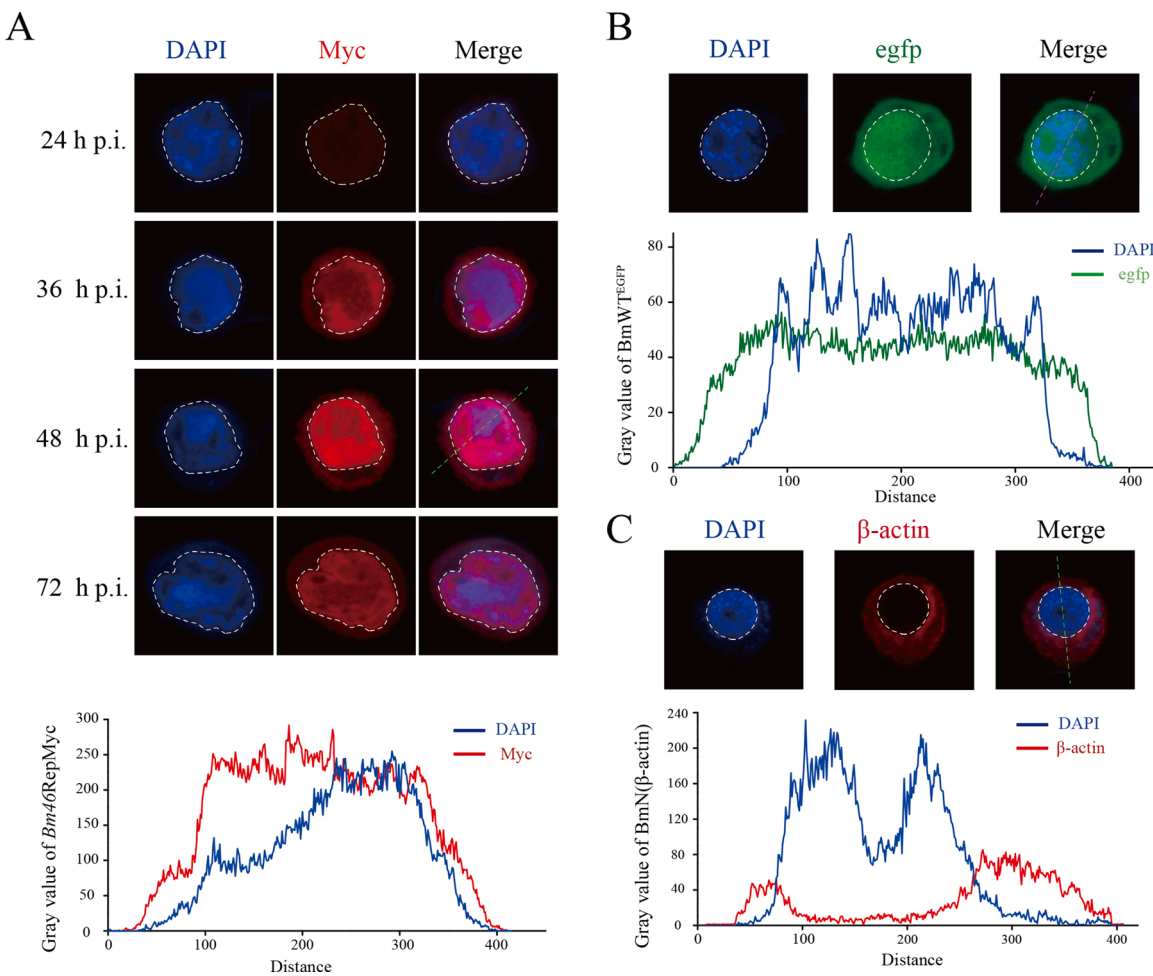


Fig. 3. Subcellular localization of Bm46 protein in infected cells. (A) At the indicated time points, BmN cells infected with *Bm46RepMyc* virus were fixed and incubated with mouse anti-Myc antibody, followed by treatment with TRITC (goat anti-mouse). 4',6-diamidino-2-phenylindole (DAPI) was used to stain the DNA of cell nucleus. Circle dashed lines indicate the border of the nucleus estimated by DAPI. From left to right: cell nucleus (DAPI; blue), Bm46-Myc (Myc; red), and merged images. The fluorescence intensity profile of the respective channel is shown in the below. (B) Subcellular localization of EGFP in infected cells. BmN cells infected with *BmWT^{EGFP}* virus (positive control). (C) Subcellular localization of β -actin. BmN cells were fixed and incubated with mouse anti- β -actin antibody (negative control).

3.2. Transcription and expression of *BmNPV Bm46* in infected cells

The *Bm46* gene codes for 161 deduced amino acid residues with a putative molecular mass of 20.7 kDa. Phylogenetic tree and alignment result revealed that it was a highly conserved gene in group I and group II NPVs (supplementary Fig. 2). Although *Bm46* was classified as an early gene based on that the *Bm46* promoter having both conserved early- and late-sequence features (Chen et al., 2013; Xue et al., 2012), the timing of *Bm46* protein expression has not been examined previously. In the present study, we investigate the temporal transcription and expression pattern of *Bm46* in BmN cells (Fig. 2). To achieve this, BmN cells were infected with *BmWT^{PH}* (wild-type) and total RNA was extracted at designated time points. Reverse-transcribed cDNAs were subjected to quantitative real-time PCR (qRT-PCR) analysis, in which 28S rRNA served as an internal control.

A *Bm46*-specific transcript was detected at 12 h post infection (p.i.), then rapidly increased during 24 h and 48 h p.i., reaching a peak at 48 h p.i. (Fig. 2C). Over a range of timings post-infection, *Bm46* protein expression was also assessed by Western blot, using α -tubulin as an internal control. However, *Bm46* protein levels were first observed at 24 h p.i., continuing to accumulate to 72 h p.i., suggesting that mRNA and protein levels may not be directly correlated at h p.i..

3.3. Subcellular localization of *Bm46*

To further probe what function *Bm46* plays in the viral life cycle, the subcellular localization of *Bm46* was analyzed using immunofluorescence microscopy. We firstly generated *Bm46RepMyc*, a C-terminal Myc-tagged of *Bm46RepMyc*. Cells infected with *Bm46RepMyc* were detected with mouse monoclonal anti-Myc and analyzed by confocal microscopy. In *Bm46RepMyc*-infected cells, *Bm46* was detected localized to the nucleus at 24 h p.i.. *Bm46* fractionated in both the nuclear and cytoplasmic fractions; however, it was more abundant in the nuclear fraction at late and very late phases (Fig. 3A). Next, immunofluorescence microscopy was carried out in *BmWT^{EGFP}*-infected cells (Fig. 3B) and no-infected cells (Fig. 3C) by detected with EGFP (positive control) and mouse anti- β -actin (negative control). These observations suggested a dynamic distribution of the *Bm46* protein throughout infection.

3.4. The *Bm46* gene is required for efficient and timely BV production

To examine the effect of the *Bm46* deletion on virus replication, BmN cells were transfected with *BmWT^{PH-EGFP}*, *Bm46KO^{PH-EGFP}* and *Bm46RepMyc^{PH-EGFP}* bacmids, and virus infections were monitored by detecting EGFP fluorescence. At 24 h post transfection (p.t.), no obvious difference in the number of fluorescent cells was observed among three viruses, indicating relatively equal transfection efficiencies (Fig. 4A). By

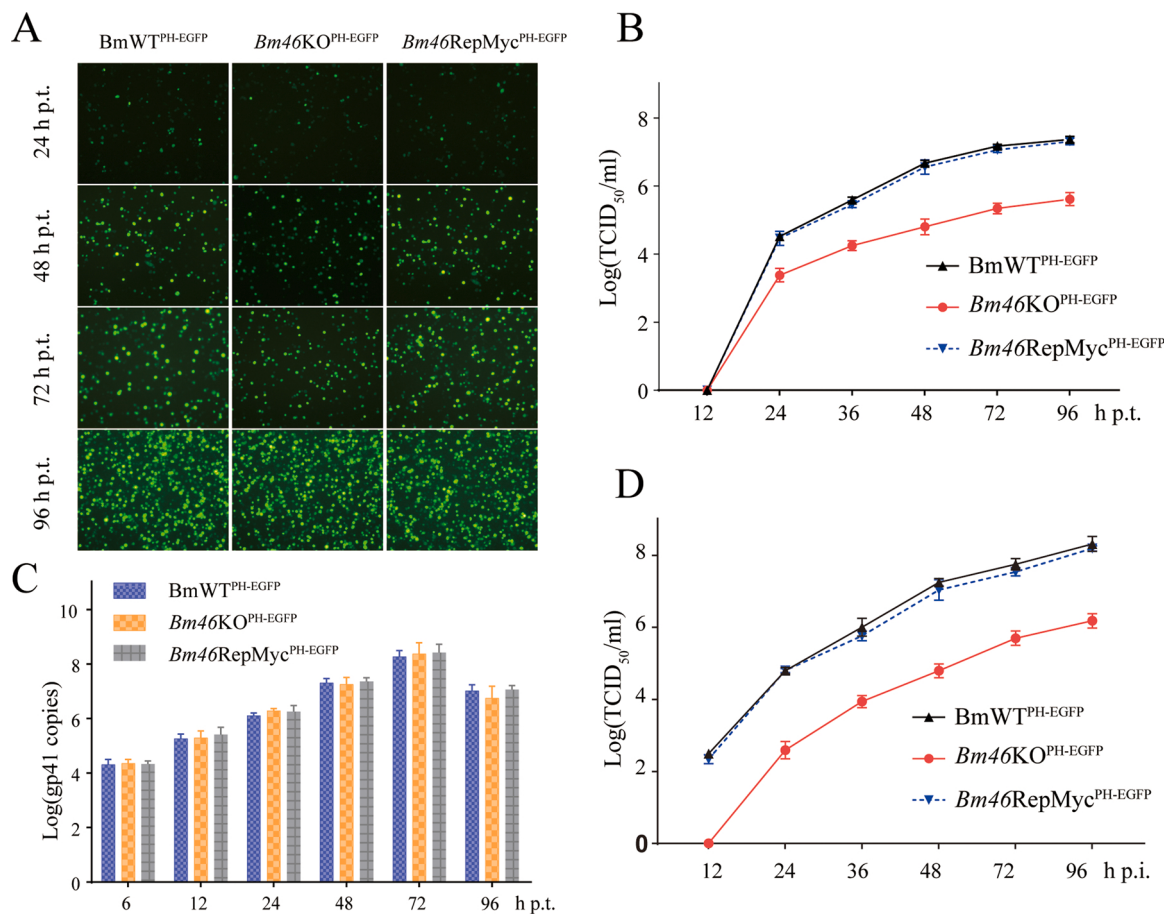


Fig. 4. Analysis of viral replication and BV production in BmN cells. (A) Transfection assay. BmN cells were transfected with bacmid DNA of BmWT^{PH-EGFP}, Bm46KO^{PH-EGFP} and Bm46RepMyc^{PH-EGFP} from 24 to 96 h p.t.. Fluorescence microscopy of viral infection progression in BmN cells after transfection was observed. (B) Viral growth curves of bacmid-transfected BmN cells. BmN cells were transfected with bacmid DNA of each virus, and the supernatant was collected at a specified time point. Titers were determined using TCID₅₀ endpoint dilution assays. Each data point was determined by three independent assays. Values above the bars indicate means and error bars represent standard deviations. (C) Quantitative Real-time PCR analysis of viral DNA synthesis. At the designated time points, total intracellular DNA was extracted and digested with *Dpn* I to eliminate bacmid DNA from *E. coli*. qRT-PCR was carried out in triplicates, and each data point was determined by the average of triplicate transfections. (D) One-step growth curve analysis of virus-infected BmN cells. BmN cells were infected with three viruses. Supernatants were harvested at the designated time points post-infection and quantified for production of infectious BV by TCID₅₀ endpoint dilution method.

72 h p.t., widespread fluorescence was observed in almost all BmWT^{PH-EGFP} and Bm46RepMyc^{PH-EGFP} transfected cells, implying that the infection had spread from the initially transfected cells. However, the number of fluorescent cells increased slightly onwards in Bm46KO^{PH-EGFP} transfected cells, suggesting that Bm46KO was capable of generating infectious BVs, but not as efficiently as BmWT^{PH-EGFP} and Bm46RepMyc^{PH-EGFP}.

Viral growth curve analysis showed that BmWT^{PH-EGFP} and Bm46RepMyc^{PH-EGFP} had similar growth trends (Fig. 4B). Infectious BV could be detected, and equivalent amounts were observed in the supernatants of BmWT^{PH-EGFP}- or Bm46RepMyc^{PH-EGFP}-transfected cells at 24 h p.t.. However, statistical analysis showed that Bm46KO^{PH-EGFP} had significantly decreased BV titers from 24 to 72 h p.i.. At 96 h p.t., the titer of Bm46KO^{PH-EGFP} was approximately 100-fold lower compared to the wildtype and rescue virus.

To further examine the effect of the Bm46 deletion on virus replication, BmN cells (1×10^6) were infected with BmWT^{PH-EGFP}, Bm46KO^{PH-EGFP} or Bm46RepMyc^{PH-EGFP} at an MOI of 1, and BV production were determined by TCID₅₀ at the indicated time points. The results of this time course analysis revealed that BV titers of both BmWT^{PH-EGFP} and Bm46RepMyc^{PH-EGFP} were comparable at each time point and reached 2.1×10^8 TCID₅₀/cell at 96 h p.i. (Fig. 4D). In contrast, the BV titer of Bm46KO increased slightly over time and was only 1.5×10^6 TCID₅₀/cell at 96 h p.i., which was more than 100-fold

lower than the BV titer of BmWT. These results indicate that Bm46 gene is not essential for viral replication but is needed for efficient BV production.

3.5. The Bm46 deletion has no effect on viral DNA replication

To determine whether Bm46 is required for viral DNA synthesis, the level of viral DNA replication in transfected cells was analyzed by qRT-PCR. The results of this analysis of Bm46KO^{PH-EGFP}, WT and Bm46RepMyc^{PH-EGFP} kept increasing up to 72 h p.i. at similar levels (Fig. 4C). These data indicated that Bm46 deletion did not result in a defect in the level of viral DNA replication.

3.6. Bm46-null mutant affects the location and expression of major viral capsid protein VP39

To investigate the reason why Bm46-null mutant affects BV production during 24–72 h p.i., we turned to examine the effect of Bm46KO on the expression and localization of the major capsid protein VP39. We performed immunofluorescence microscopy using an antibody against VP39 (Fig. 5A). At 24 h p.i., VP39 showed punctate localization to the VS in both BmWT- and Bm46KO-infected cells. At 36 h p.i., however, while BmWT-infected cells continued to show punctate or diffused VP39 localization in the VS, the majority of Bm46KO-infected cells had VP39

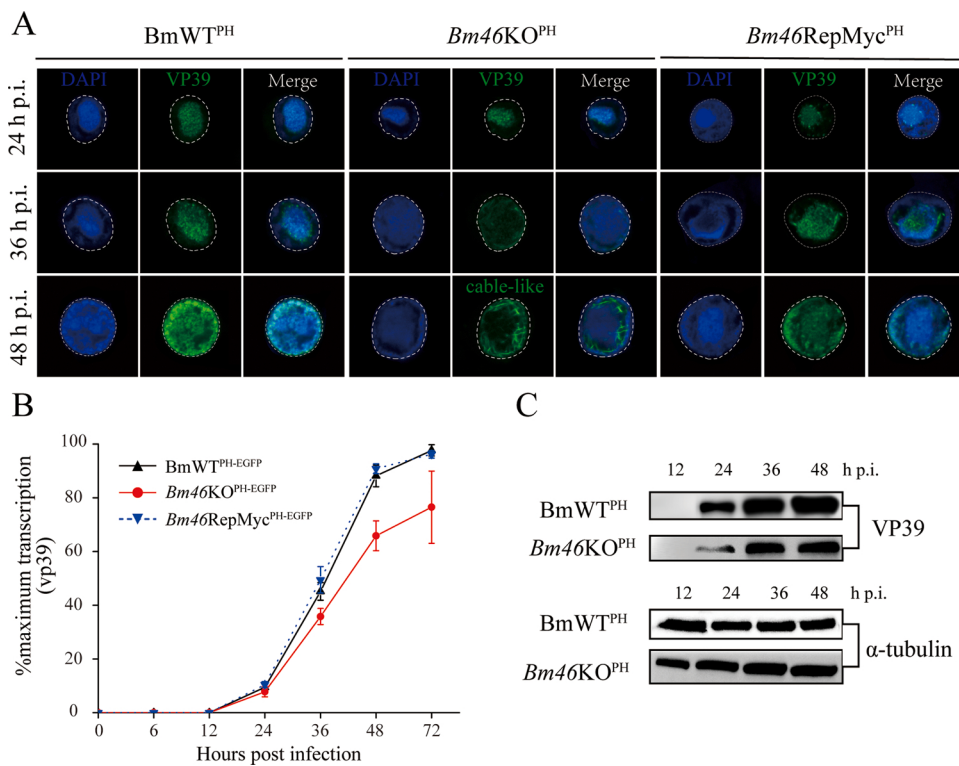


Fig. 5. Bm46 is essential for the major capsid protein VP39 localization and affects its expression. (A) BmN cells infected with BmWT^{PH}, Bm46KO^{PH} or Bm46RepMyc^{PH} at an MOI of 1 and fixed at the indicated time points. After incubation with rabbit monoclonal anti-VP39, the infected cells were treated with FITC (green; goat anti-rabbit) and DAPI (blue). (B, C) Effect of Bm46 null on the expression of VP39. Two sets of BmN cells infected with BmWT^{PH} or Bm46KO^{PH} at an MOI of 1 were used for total RNA or protein extraction and analyzed by real-time PCR or western blot to determine VP39 mRNA and protein levels, respectively. The center bar represents the mean, and the top and bottom bars represent the SD. P-values were calculated using a Student *t* test, p-value < 0.05.

in the RZ. At 48 h.p.i., VP39 redistributed to a punctate localization in the whole nucleus in BmWT-infected cells, whereas it remained filamentous in the ring zones of most Bm46KO-infected cells, where it assembled into long cables.

Quantitative real-time RT-PCR analyses revealed that Bm46-null resulted in 22.7 % lower vp39 mRNA level at 72 h.p.i. (Fig. 5B), which compared to cells infected with BmWT^{PH} or Bm46RepMyc^{PH}. Consisting with Western blot result (Fig. 5C), the expressions of VP39 protein were reduced from 24 h.p.i. to 72 h.p.i.

3.7. Transmission electron microscopy analysis

To elucidated the roles of Bm46, we examined the effect of the Bm46KO mutation on nuclear organization and nucleocapsid assembly. We applied transmission electron microscopy (TEM) to compare intra-nuclear structures in BmWT, Bm46KO and Bm46RepMyc-transfected cells, and BmWT^{PH}, Bm46KO^{PH} and Bm46RepMyc. At 36 h.p.i., both BmWT- and BmWT^{PH}-transfected cells showed a condensed stroma (VS), composed of electron-dense lobes, a peripheral RZ, nucleocapsid-enveloped ODVs and OBs, both of which contained rod-shaped nucleocapsids (Fig. 6A,7A). In contrast, both Bm46KO- and Bm46KO^{PH}-transfected cells lacked a well-defined VS, instead containing a more amorphous region that occupied most of the nucleus and devoid of electron-dense lobes or visible nucleocapsids (Fig. 6B,7A). Moreover, in partial enlarged views, the peripheral RZ was densely packed with long tubular structures that were variable in length and were often bundled or clustered (Fig. 6B). Thus, the Bm46KO mutation causes aberrant assembly of VP39 into filamentous structures during late stage of transfection. In addition, the polyhedra from Bm46KO^{PH}-transfected cells appeared to contain fewer ODVs in comparison to BmWT^{PH} in enlarged views. The tubules also varied in electron density, with some being nearly electron-lucent and others having electrodense areas indicating the viral DNA packaging.

Taken together with the VP39 immunofluorescence microscopy studies, these results suggest that the tubular structures are aberrant assemblies of VP39 that failed to form into unit-length nucleocapsids but

instead assembled into elongated tubular structures that contain viral DNA occasionally.

3.8. Bm46 knockout impaired the embedding of ODV into polyhedra

After displayed Bm46KO-infected cells, we purified OBs from BmWT^{PH}-, Bm46KO^{PH}- and Bm46RepMyc^{PH}-infected larvae and analyzed them by transmission electron microscopy. Upon closer observations under TEM, the numbers of embedding ODVs appeared to be less than that of the control virus (Fig. 7B).

We firstly examined the production of occlusion bodies and the number of occlusion bodies was not affected upon infection with Bm46KO^{PH} using hemocytometer counting (Fig. 7C). We next performed DNA extractions from 5×10^8 OBs and proceeded to Kruskal-Wallis and Mann-Whitney nonparametric analyses. No significant differences in the mean amounts (\pm standard deviations) of DNA in OBs were detected between the BmWT^{PH} (430.9 ± 12.7 ng/ μ l) and Bm46RepFlag^{PH} (424.4 ± 11.4 ng/ μ l). However, Bm46-null OBs yielded 33.4 % less DNA, with 286.8 ± 26.9 ng/ μ l obtained from 5×10^8 OBs, representing an approximately 1.5-fold reduction in OBs DNA content (Fig. 7D).

To further analyze the effect of Bm46 deletion on ODV embedding, we quantified viral genome copies by qRT-PCR. As shown in Fig. 7E, the genomic DNA content extracted from OBs of BmWT^{PH} and Bm46RepMyc^{PH} exhibited the same level. However, Bm46-null resulted in 30 % lower viral genome DNA copies of OBs.

3.9. Bm46 deletion does not affect nuclear actin polymerization and localization

It has been demonstrated that F-actin polymerization is required for nucleocapsid assembly (Goley et al., 2006). AcMNPV infected Sf9 cells treated with CD (Hess et al., 1989), is capable of binding specifically to the growing end of the actin filament, resulting in a failure of viral morphogenesis. We hypothesized that the location of VP39 from the VS to RZ might be associated with the actin polymerization. To verify this, the distribution of actin in Bm46KO-infected cells was investigated using

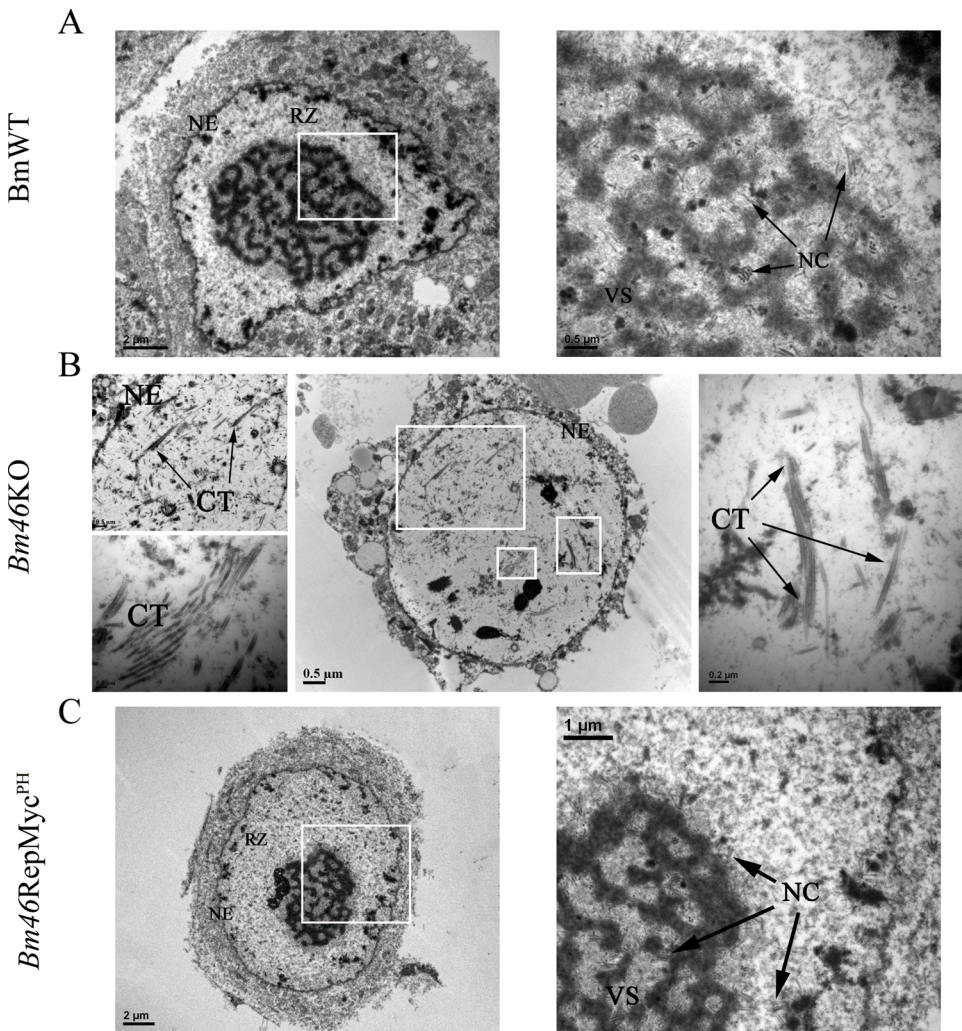


Fig. 6. TEM analysis of BmN cells transfected with bacmid DNA of BmWT, *Bm46KO* and *Bm46RepMyc*. (A, C) Electron micrographs of BmN cells transfected with BmWT or *Bm46RepMyc*, fixed at 36 h p.t., and prepared for TEM. The nuclear envelope (NE), ring zone (RZ), and virogenic stroma (VS) are indicated. Magnified view of the boxed area showing individual nucleocapsids (NC). (B) Electron micrographs of BmN cells transfected with *Bm46KO*, as in panel A. The nuclear envelope (NE), ring zone (RZ), and virogenic stroma (VS) are indicated. Magnified view of the boxed area from middle showed capsid-like tubule structures (CT), indicating aggregates of capsid-like tubule structures (CT), in a longitudinal section.

immunofluorescence assays (Fig. 8A). The distribution patterns of actin were similar in those observed in *Bm46KO*- or BmWT-infected cells, suggesting that *Bm46* deletion exerted no significant effect on the actin localization (Fig. 8B).

4. Discussion

BmNPV orf 46 and its homologues are highly conserved genes in group I and group II, but their biological functions remain elusive. Although it was proposed to classify *Bm46* as an early gene based on early and late promoter motifs, our results revealed that *Bm46* played some certain roles in late infection, and its deletion resulted in the formation of abnormally elongated capsid structures and reduced BV production.

Based on a previous report, Ono et al. generated a series of gene mutant BmNPVs for 141 genes (Ono et al., 2012). And the *Bm46* gene was regarded as type-A knockout BmNPVs, which were able to produce infectious progeny virus. However, our results demonstrated that *Bm46* was not an essential gene for virus replication, but was required for efficient levels of BV production, since its deletion resulted in a decrease in levels of BV production from 24 to 96 h p.t.. These discrepancies may be caused by the difference in length of the deletion, the location of the deletion region, and other effects. Although it has been reported that *Ha50*, a *Bm46* homolog of the *Helicoverpa armigera* nucleopolyhedrovirus (HearNPV), is not essential (Chen et al., 2012). Nevertheless, our results revealed that BV production was reduced by the deletion of

Bm46, suggesting that these homologs played somewhat different roles in the infection cycle of the corresponding virus.

Thus, it is necessary to take a thorough assessment on the role of *Bm46* throughout infection. Our findings demonstrated that *Bm46* was expressed predominantly at late stage, with detectable protein first observed at 24 h p.i.. However, *Bm46* transcript was firstly detected at 12 h p.i., suggesting that mRNA and protein levels may not be directly correlated at later time points, indicating that *Bm46* may play a role in the late infection. It is likely that *Bm46* may involve in other activities of viral life, such as proper capsid assembly or virion maturation, the efficient transport of nucleocapsids from the nucleus to the cytoplasm, or virus budding from the cell (Garoff et al., 1998).

Therefore, to further investigate the role of *Bm46* gene in the late infection, we started with the effect of reduced BV titer. The defects in BV production could be caused by defective virus egress; impaired nucleocapsid structure integrity; or alterations in the transport of nucleocapsids within cells, packaging, or virus assembly (Wu and Passarelli, 2012). Our finding demonstrated that the lack of *Bm46* gene appeared to affect the expression of capsid protein VP39 in both mRNA and protein level. *Bm46* is also important for nucleocapsid morphogenesis. Electron microscopy revealed that the abnormal electron-dense bodies were found in the VS upon *Bm46* deletion, and aberrant capsid-like tubular structures accumulated in the RZ. In addition, empty capsid structures and fewer ODV embedding into OBs were also observed in cells transfected with *Bm46KO*^{PH}.

Furthermore, cells were transfected/infected with mutant bacmids/

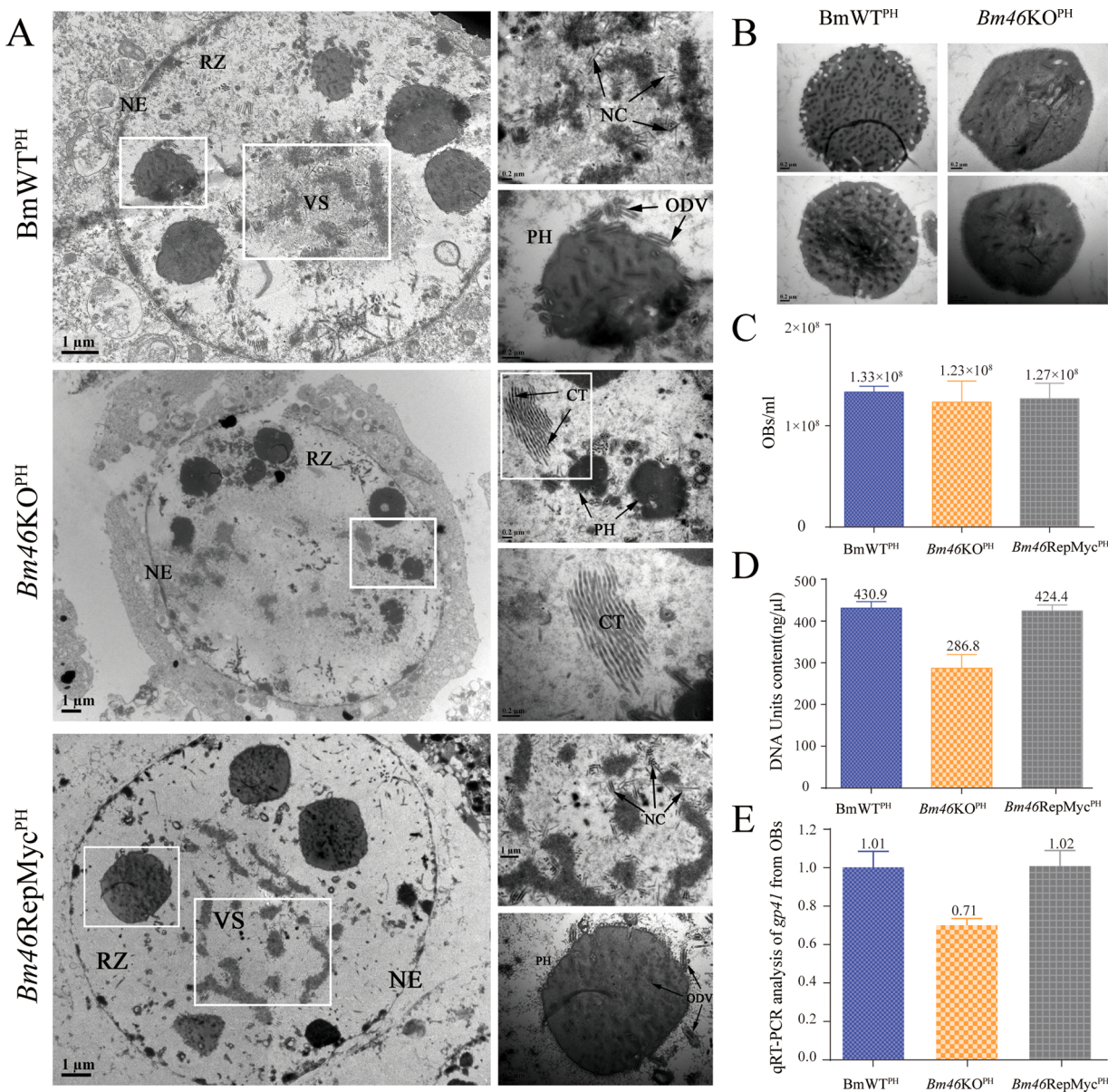


Fig. 7. TEM analysis of infected BmN cells, OBs from larvae and comparison of viral genome DNA. (A) Electron micrographs of BmN cells infected with BmWT^{PH}, Bm46KO^{PH} or Bm46RepMyc^{PH} fixed at 48 h p.t. and prepared for TEM. (B) OBs purified from the infected larvae were observed by TEM. The corresponding virus names of OBs were indicated on the left. (C) Analysis the production of OBs. The released OBs from the infected BmN cells was harvested at 168 h p.i. and counted using hemocytometer. (D) Mean amounts of DNA extracted from 5×10^8 OBs of BmWT^{PH}, Bm46KO^{PH}, or Bm46RepMyc^{PH}. (E) The comparison of viral genome DNA from 5×10^8 OBs of three recombinant viruses by qRT-PCR. Each data point represents the average of triplicate determinations. Values above the bars indicate means, and error bars indicate standard deviations.

viruses carrying deletions of pk-1/ac10(Liang et al., 2013), ac53(Liu et al., 2008), VP1054/ac54(Guan et al., 2016; Marek et al., 2013), vlf-1/ac77(Vanarsdall et al., 2006), 38 K/ac98(Lai et al., 2018), or ac102(Hepp et al., 2018), which were important for nucleocapsid assembly. The appearance of elongated tubular structure was consistent with the immunofluorescence microscopy images showing that VP39 mislocalized into filaments and cables in the RZ of Bm46KO^{PH}-infected cells. Therefore, these data confirmed that Bm46 was essential for the proper nucleocapsid morphogenesis and ODV occlusion.

In addition, electron microscopy observation also showed that the deletion of Bm46 had a remarkable effect on OBs with fewer ODVs, which was confirmed by measurement of a lower viral DNA content. qRT-PCR and Western blot analysis showed that a decrease in the average amount of DNA per OB and reduced amounts of VP39 in Bm46 deleted BmNPV mutants, indicating that Bm46 knockout disrupted the

normal assembly of nucleocapsids and therefore affected ODV occlusion.

BmNPV belongs to a diverse group of viral and bacterial pathogens that target the host cell actin cytoskeleton during infection. Actin polymerization can be induced by BmNPV to facilitate the infection of host cells(Goley et al., 2006). Nuclear actin assembly by P78/83 (Machesky et al., 2001) and host Arp2/3 complex is essential for viral progeny production.

Current studies generally focus on complete understanding of viral protein complexes containing ODV-EC27, BV/ODV-C42 (C42; encoded by *ac101*), Ac102 and P78/83(Braunagel et al., 2001), which are associated with one end of the nucleocapsid(Hepp et al., 2018; Russell et al., 1997). Although we have observed nuclear F-actin in late-stage Bm46KO-infected cells, we could not exclude the possibility that Bm46 deletion would exerted a minor influence on nuclear F-actin that escaped detection by phalloidin staining, which may lead to the final

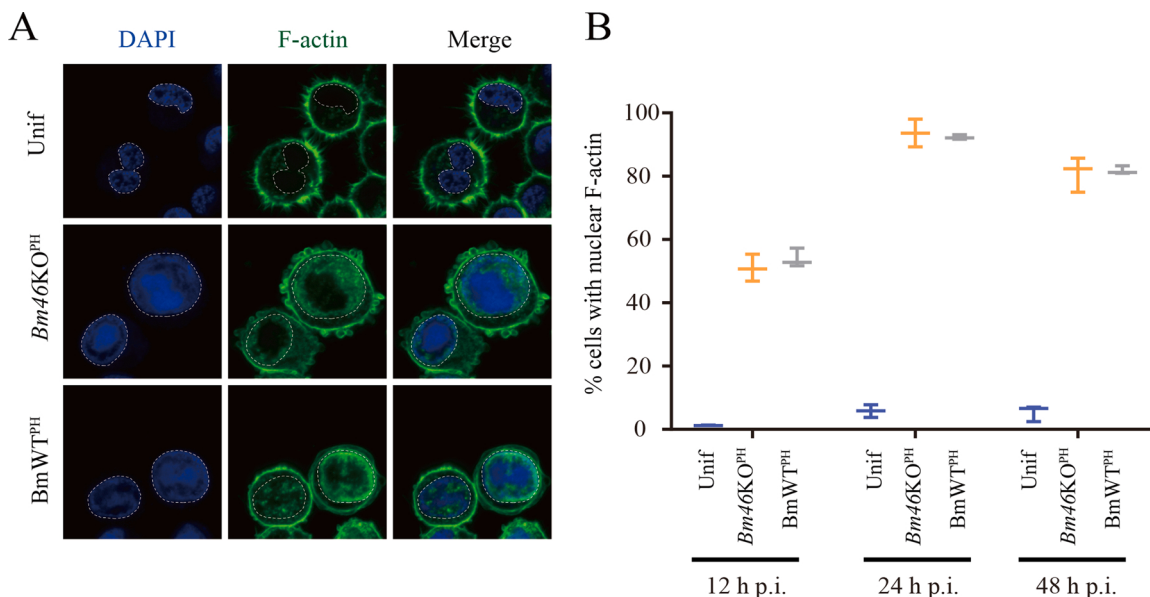


Fig. 8. Subcellular localization of F-actin in BmN cells infected with recombinant viruses. (A) BmN cells infected with $BmWT^{PH}$ or $Bm46KO^{PH}$ virus at an MOI of 1, fixed at 36 h p.i., and stained for F-actin (Alexa Fluor-phalloidin; green), and DNA (DAPI; blue). (B) Quantification of the percent cells with nuclear F-actin at 12, 36, and 48 h p.i., defined as cells with detection of nuclear F-actin intensity, using Image J software, from Phalloidin-FITC staining. Each dot represents the average percentage of cells containing nuclear actin for one independent experiment. Lines indicate the means for three independent experiments.

reduced BV production to a certain extent.

In conclusion, our findings showed that the deletion of *Bm46* gene resulted in a decrease in BV production but did not affect viral DNA replication. In addition, *Bm46* gene played an important role in nucleocapsid assembly and morphogenesis where *Bm46*-mutant gave rise to the aggregation of capsid-like tubule at the periphery of the nucleus. Moreover, *Bm46*-null impacted capsid protein VP39 expression and distribution, leading to a “filamentous” or “cable-like” pattern. These findings enrich our understanding on nucleocapsid formation and virus assembly. Further research is required to disclose the formative mechanism of aberrant long electron-lucent tubular structures for *Bm46* knockout. Meanwhile, it is also an interesting scientific issue to further investigate about baculovirus nucleocapsid assembly, which could be conducive to understanding baculovirus life cycle.

Author contributions

X.F.W conceived and designed the experiments; Y.L and J.J.Z performed the experiments; Y.L processed the data and wrote the manuscript. X.S.K, N.C and X.Q.Z reviewed the manuscript.

Declaration of Competing Interest

The authors reported no declarations of interest.

Acknowledgements

We thank Associate Professor Lijian Luo (Zhejiang University) and Dr. Weifan Xu for reading the manuscript and giving suggestions. We are also grateful to Yunqin Li and Li Xie for professional technical support in the Bio-ultrastructure analysis Lab of Analysis Center of Zhejiang University.

This study was supported by the National Natural Science Foundation of China (project 31772675 and 31972619) and the Natural Science Foundation of Zhejiang Province (Z20C170008). We declare that there is no conflict of interest in our work. All the experiments involving animals were conducted in strict accordance with the Institutional Animal Care and Use Committee of Zhejiang University.

Appendix A. Supplementary data

Supplementary material related to this article can be found, in the online version, at doi:<https://doi.org/10.1016/j.virusres.2020.198145>.

References

- Braunagel, S.C., Summers, M.D., 2007. Molecular biology of the baculovirus occlusion-derived virus envelope. *Curr. Drug Targets* 8 (10), 1084–1095.
- Braunagel, S.C., Guidry, P.A., Rosas-Acosta, G., Engelking, L., Summers, M.D., 2001. Identification of BV/ODV-C42, an *Autographa californica* nucleopolyhedrovirus *orf101*-encoded structural protein detected in infected-cell complexes with ODV-EC27 and p78/83. *J. Virol.* 75 (24), 12331–12338.
- Charter, C., Degryse, E., Gantzer, M., Dieterle, A., Pavirani, A., Mehtali, M., 1996. Efficient generation of recombinant adenovirus vectors by homologous recombination in *Escherichia coli*. *J. Virol.* 70 (7), 4805–4810.
- Chen, Y., Zheng, F., Tao, L., Zheng, Z., Liu, Y., Wang, H., 2012. *Helicoverpa armigera* nucleopolyhedrovirus ORF50 is an early gene not essential for virus propagation *in vitro* and *in vivo*. *Virus Genes* 45 (1), 149–160.
- Chen, Y.-R., Zhong, S., Fei, Z., Hashimoto, Y., Xiang, J.Z., Zhang, S., Blissard, G.W., 2013. The transcriptome of the baculovirus *Autographa californica* multiple nucleopolyhedrovirus in *Trichoplusia ni* cells. *J. Virol.* 87 (11), 6391–6405.
- Garoff, H., Hewson, R., Opstelten, D.-J.E., 1998. Virus maturation by budding. *Microbiol. Mol. Biol. Rev.* 62 (4), 1171–1190.
- Goley, E.D., Ohkawa, T., Mancuso, J., Woodruff, J.B., D'Alessio, J.A., Cande, W.Z., Volkman, L.E., Welch, M.D., 2006. Dynamic nuclear actin assembly by Arp2/3 complex and a baculovirus WASP-like protein. *Science* 314 (5798), 464–467.
- Gomi, S., Majima, K., Maeda, S., 1999. Sequence analysis of the genome of *Bombyx mori* nucleopolyhedrovirus. *J. Gen. Virol.* 80 (Pt 5)(5), 1323–1337.
- Guan, Z., Zhong, L., Li, C., Wu, W., Yuan, M., Yang, K., 2016. The *Autographa californica* multiple nucleopolyhedrovirus ac54 gene is crucial for localization of the major capsid protein VP39 at the site of nucleocapsid assembly. *J. Virol.* 90 (8), 4115–4126.
- Hanahan, D., 1983. Studies on transformation of *Escherichia coli* with plasmids. *J. Mol. Biol.* 166 (4), 557–580.
- Hayakawa, T., Ko, R., Okano, K., Seong, S.I., Goto, C., Maeda, S., 1999. Sequence analysis of the *Xestia c-nigrum* granulovirus genome. *Virology* 262 (2), 277–297.
- Hepp, S.E., Borgo, G.M., Ticau, S., Ohkawa, T., Welch, M.D., 2018. Baculovirus AC102 is a nucleocapsid protein that is crucial for nuclear actin polymerization and nucleocapsid morphogenesis. *J. Virol.* 92 (11).
- Herniou, E.A., Luque, T., Chen, X., Vlak, J.M., Winstanley, D., Cory, J.S., O'Reilly, D.R., 2001. Use of whole genome sequence data to infer baculovirus phylogeny. *J. Virol.* 75 (17), 8117–8126.
- Herniou, E.A., Olszewski, J.A., Cory, J.S., O'Reilly, D.R., 2003. The genome sequence and evolution of baculoviruses. *Annu. Rev. Entomol.* 48 (1), 211–234.
- Hess, R.T., Goldsmith, P.A., Volkman, L.E., 1989. Effect of cytochalasin D on cell morphology and AcMNPV replication in a *Spodoptera frugiperda* cell line. *J. Invertebr. Pathol.* 53 (2), 169–182.

- Jehle, J.A., Blissard, G., Bonning, B., Cory, J., Herniou, E., Rohrmann, G., Theilmann, D., Thiem, S., Vlak, J., 2006. On the classification and nomenclature of baculoviruses: a proposal for revision. *J. Arch. Virol.* 151 (7), 1257–1266.
- Lai, Q., Wu, W., Li, A., Wang, W., Yuan, M., Yang, K., 2018. The 38K-Mediated specific dephosphorylation of the viral core protein P6.9 plays an important role in the nucleocapsid assembly of *Autographa californica* multiple nucleopolyhedrovirus. *J. Virol.* 92 (9).
- Liang, C., Li, M., Dai, X., Zhao, S., Hou, Y., Zhang, Y., Lan, D., Wang, Y., Chen, X., 2013. *Autographa californica* multiple nucleopolyhedrovirus PK-1 is essential for nucleocapsid assembly. *Virology* 443 (2), 349–357.
- Liu, C., Li, Z., Wu, W., Li, L., Yuan, M., Pan, L., Yang, K., Pang, Y., 2008. *Autographa californica* multiple nucleopolyhedrovirus ac53 plays a role in nucleocapsid assembly. *Virology* 382 (1), 59–68.
- Luckow, V.A., Lee, S., Barry, G., Ollins, P., 1993. Efficient generation of infectious recombinant baculoviruses by site-specific transposon-mediated insertion of foreign genes into a baculovirus genome propagated in *Escherichia coli*. *J. Virol.* 67 (8), 4566–4579.
- Machesky, L.M., Insall, R.H., Volkman, L.E., 2001. WASP homology sequences in baculoviruses. *Trends Cell Biol.* 11 (7), 286–287.
- Maeda, S., Kawai, T., Obinata, M., Fujiwara, H., Horiuchi, T., Saeki, Y., Sato, Y., Furusawa, M., 1985. Production of human α -interferon in silkworm using a baculovirus vector. *Nature* 315 (6020), 592–594.
- Marek, M., Romier, C., Galibert, L., Merten, O.-W., van Oers, M.M., 2013. Baculovirus VP1054 is an acquired cellular PUR α , a nucleic acid-binding protein specific for GGN repeats. *J. Virol.* 87 (15), 8465–8480.
- Miao, X.X., Xub, S.J., Li, M.H., Li, M.W., Huang, J.H., Dai, F.Y., Marino, S.W., Mills, D.R., Zeng, P., Mita, K., Jia, S.H., Zhang, Y., Liu, W.B., Xiang, H., Guo, Q.H., Xu, A.Y., Kong, X.Y., Lin, H.X., Shi, Y.Z., Lu, G., Zhang, X., Huang, W., Yasukochi, Y., Sugasaki, T., Shimada, T., Nagaraju, J., Xiang, Z.H., Wang, S.Y., Goldsmith, M.R., Lu, C., Zhao, G.P., Huang, Y.P., 2005. Simple sequence repeat-based consensus linkage map of *Bombyx mori*. *Proc. Natl. Acad. Sci. U. S. A.* 102 (45), 16303–16308.
- Ono, C., Kamagata, T., Taka, H., Sahara, K., Asano, S., Bando, H., 2012. Phenotypic grouping of 141 BmNPVs lacking viral gene sequences. *Virus Res.* 165 (2), 197–206.
- Rohrmann, G.F., 2013. Baculovirus Molecular Biology.
- Russell, R., Funk, C., Rohrmann, G., 1997. Association of a baculovirus-encoded protein with the capsid basal region. *Virology* 227 (1), 142–152.
- Simón, O., Williams, T., Asensio, A.C., Ros, S., Gaya, A., Caballero, P., Possee, R.D., 2008. Sf29 gene of *Spodoptera frugiperda* multiple nucleopolyhedrovirus is a viral factor that determines the number of virions in occlusion bodies. *J. Virol.* 82 (16), 7897–7904.
- Vanarsdall, A.L., Okano, K., Rohrmann, G.F., 2005. Characterization of the replication of a baculovirus mutant lacking the DNA polymerase gene. *Virology* 331 (1), 175–180.
- Vanarsdall, A.L., Okano, K., Rohrmann, G.F., 2006. Characterization of the role of very late expression factor 1 in baculovirus capsid structure and DNA processing. *J. Virol.* 80 (4), 1724–1733.
- Wu, W., Passarelli, A.L., 2012. The *Autographa californica* M nucleopolyhedrovirus ac79 gene encodes an early gene product with structural similarities to UvrC and intron-encoded endonucleases that is required for efficient budded virus production. *J. Virol.* 86 (10), 5614–5625.
- Xu, W., Fan, Y., Wang, H., Feng, M., Wu, X., 2019. *Bombyx mori* nucleopolyhedrovirus F-like protein Bm14 affects the morphogenesis and production of occlusion bodies and the embedding of ODVs. *Virology* 526, 61–71.
- Xue, J., Qiao, N., Zhang, W., Cheng, R.-L., Zhang, X.-Q., Bao, Y.-Y., Xu, Y.-P., Gu, L.-Z., Han, J.-D.J., Zhang, C.-X., 2012. Dynamic interactions between *Bombyx mori* nucleopolyhedrovirus and its host cells revealed by transcriptome analysis. *J. Virol.* 86 (13), 7345–7359.